

Shape from shading and polarization constrained by approximate shape

Wataru Muraoroshi Daisuke Miyazaki
Hiroshima City University

3-4-1 Otsukahigashi, Asaminami-ku, Hiroshima city, 731-3194 JAPAN
{ c20206 (at) e., miyazaki (at) } hiroshima-cu.ac.jp

Abstract

We propose a method which estimates the surface normal from shading information and polarization information. Unlike photometric stereo techniques which use three lights, shape-from-shading uses a single light and is an ill-posed problem. Therefore, to uniquely determine the surface normal using a shape-from-shading method, additional assumptions or additional inputs are required. We use polarization for additional input, because polarization can constrain the surface normal. One example of common assumption is to limit the target object to be a single color, but such assumption restricts the application field. Therefore, we use an approximate shape of the object to solve this problem. Thanks to this approximate shape, we can estimate the surface normal of multi-colored object.

1 Introduction

Shape-from-shading, which uses a single image, is an ill-posed problem, and thus, existing methods [1, 2, 3] used additional assumptions, additional inputs, or training data to solve the problem. Polarization is also useful for estimating surface normal. A small number of method obtains the surface normal from shading and polarization under a single light. Most of them assume a single-colored object for target objects, while we overcome this problem using an approximate shape of the object as a cue. Thanks to this additional information, our method (Fig. 1) can be applied to multi-colored objects.

Shape-from-shading [1, 2, 3, 4, 5, 6], which use a single image, is an ill-posed problem. Polarization [7] is also useful for estimating the surface normal of objects, and polarization is used for photometric stereo [8, 9, 10, 11, 12, 13] and shape-from-shading [15, 16, 17, 14]. These methods [15, 16, 17] used the degree of polarization; however, the degree of polarization depends on the index of refraction and surface roughness. Previous work [14] did not use the degree of polarization but used the phase angle of polarization, because it is independent to the index of refraction nor surface roughness. Because the phase angle of polarization solely cannot determine the surface normal, shading information is also used where the light source is set almost next to the camera. The previous method

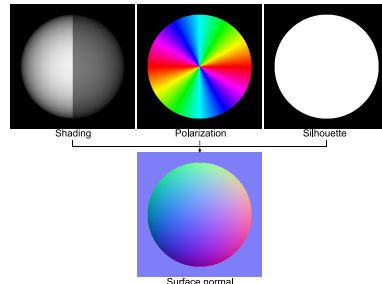


Figure 1. Proposed method: Shape from shading, polarization, and silhouette.

determined the albedo as the maximum brightness of the object because the surface normal heading to the light source has the same brightness as the albedo if the object is single colored. In order to overcome this problem, we use an approximate shape, which is calculated from the silhouette of the object. We prove that our method can estimate the surface normal of the object which has multiple colors.

2 Shape from shading, silhouette, or polarization

Under the condition that the object obeys the Lambertian reflection model and the light source is an infinite-far single light, the observed brightness i can be represented as follows.

$$i = \rho \mathbf{n} \cdot \mathbf{l}. \quad (1)$$

The unit vector $\mathbf{l} = (l_x, l_y, l_z)^\top$ represents the light source direction. The surface normal is represented as the unit vector $\mathbf{n} = (n_x, n_y, n_z)^\top$. The reflectance of diffuse reflection (hereafter, albedo) is denoted ρ .

Assuming that the light source direction is given, we have three unknowns, ρ , n_x , and n_y . Note that n_z is automatically obtained from $n_z = \sqrt{1 - n_x^2 - n_y^2}$. Since shape-from-shading has one constraint (Eq. (1)), we need additional two information to determine all three parameters. Two information are silhouette and polarization. The detailed process of using these three information is described in Section 3.

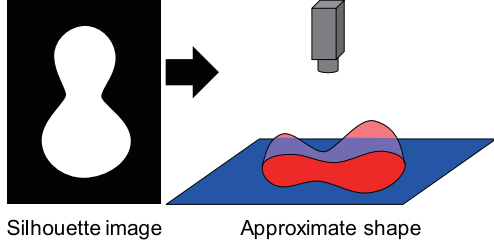


Figure 2. Approximate shape obtained from silhouette.

Suppose that we have detected the pixel positions of the object boundary in the image plane (Fig. 2). Using this single image, the approximate shape of the object can be obtained from the silhouette. The details of this shape is far from the true shape, however, it is approximately similar to the true shape. We denote the surface normal of such shape obtained from silhouette as guide normal in this paper. We skip to explain the algorithm to calculate guide normal since its implementation detail is relatively not important. The guide normal can be obtained solely from a single image. Since the guide normal is different from true normal, we need a further process (Section 3) to obtain the true normal.

We project unpolarized light onto the object and observe the diffusely reflected light passing through the polarizer. Illuminated light penetrated into the object randomly reflects inside the object. The light becomes unpolarized during the random reflection inside the object. The unpolarized light inside the object partially polarizes when the light transmits to the air.

The polarization effect can be expressed by transmissivity. Transmissivity T_p parallel to reflection plane is shown in Eq. (2), and transmissivity T_s perpendicular to reflection plane is shown in Eq. (3). The reflection plane is a plane which includes the surface normal and the viewing direction.

$$T_p = \frac{\sin 2\theta_1 \sin 2\theta_2}{\sin^2(\theta_1 + \theta_2) \cos^2(\theta_1 - \theta_2)}, \quad (2)$$

$$T_s = \frac{\sin 2\theta_1 \sin 2\theta_2}{\sin^2(\theta_1 + \theta_2)}. \quad (3)$$

Here, the angle between the surface normal and the viewer direction is denoted as θ_1 , and the angle between the incident direction and the opposite of the surface normal is denoted as θ_2 . As for dielectric objects, Eq. (4) holds.

$$T_p \geq T_s \quad (4)$$

Due to this property, the observed intensity of diffuse reflection is partially polarized. The maximum light (T_p) is observed when the polarizer angle coincide with the orientation of the reflection plane (Fig. 3). In

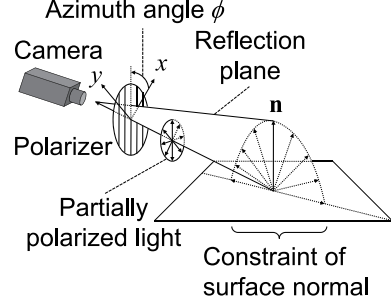


Figure 3. Relationship between the surface normal and the reflection plane.

this paper, the polarizer angle at which I_{\max} is observed is referred to as the phase angle ϕ .

The surface normal is represented in polar coordinates, where the azimuth angle is denoted ϕ and the zenith angle is denoted θ . Figure 3 shows that the azimuth angle is the same as the phase angle. However, the azimuth angle calculated from the polarization has 180° -ambiguity because a linear polarizer has a 180° cycle. Thus, the azimuth angle of the surface normal will be either ϕ or $\phi + 180^\circ$.

3 Shape from shading, silhouette, and polarization

We assume that the light source and the camera are in almost the same location. Our method allows the object to be multi-colored, thus the albedo ρ is not uniform. First of all, we use the guide normal (Section 2) in order to estimate the albedo ρ . From the guide normal $\tilde{\mathbf{n}} = (\tilde{n}_x, \tilde{n}_y, \tilde{n}_z)^\top$, and the light direction $\mathbf{l} = (0, 0, 1)^\top$, Eq. (1) becomes as follows.

$$\tilde{\rho} = \frac{i}{\tilde{n}_z} \quad (5)$$

Guide normal $\tilde{\mathbf{n}}$ is slightly different from the true normal, and thus, the estimated albedo $\tilde{\rho}$ (Eq. (5)) is slightly different from the true albedo. In order to reduce the estimation error of albedo, we applied median filter to it, and we denote the output of median filtering applied to $\tilde{\rho}$ as ρ .

Since the light source direction is the same as that of the camera, the z value of the surface normal can be obtained as follows.

$$n_z = \frac{i}{\rho} \quad (6)$$

The azimuth angle obtained from polarization has 180° -ambiguity (Section 2). Thus, surface normal and azimuth angle ϕ are related as follows.

$$(n_x, n_y) = \sqrt{1 - n_z^2} (\cos(\phi), \sin(\phi)), \quad (7)$$

$$(n_x, n_y) = \sqrt{1 - n_z^2} (\cos(\phi + \pi), \sin(\phi + \pi)). \quad (8)$$

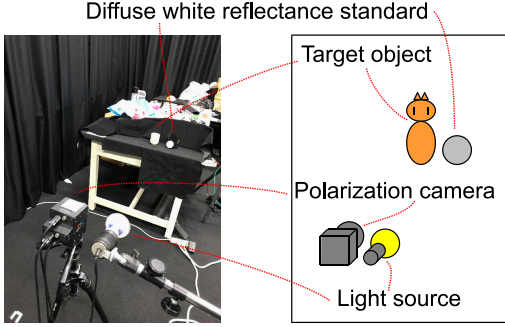


Figure 4. Experimental environment.

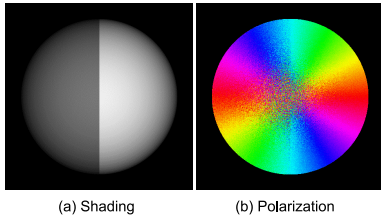


Figure 5. Simulationaly generated input data: (a) Target object and (b) azimuth angle with ambiguity.

Two possible candidates of the surface normal are calculated from Eqs. (7)–(8), i.e., either ϕ or $\phi + 180^\circ$ is the correct azimuth angle (Section 2). We use the guide normal \tilde{n}_x and \tilde{n}_y (Section 2) to uniquely determine the azimuth angle ϕ or $\phi + 180^\circ$ in the range between 0 to 360° . Eq. (9) shows the dot product between the (x, y) component of the surface normal of guide normal and the orientation which represents the azimuth angle ϕ , while Eq. (10) shows the dot product between the guide normal and the azimuth angle $\phi + 180^\circ$.

$$A_\phi = \tilde{n}_x \cos \phi + \tilde{n}_y \sin \phi, \quad (9)$$

$$A_{\phi+\pi} = \tilde{n}_x \cos(\phi + \pi) + \tilde{n}_y \sin(\phi + \pi). \quad (10)$$

Note that, the angle between two vectors are smaller than 90° if the dot product is positive, and that are greater than 90° if it is negative. If $A_\phi \geq A_{\phi+\pi}$, we determine the surface normal as Eq. (7). If $A_{\phi+\pi} \geq A_\phi$, we determine the surface normal as Eq. (8).

4 Experiments

The experiments are performed in a dark room (Fig. 4). The light source is placed close to the camera. The polarization camera captures the linear polarization parameters in a single shot.

4.1 Performance evaluation

First of all, we analyzed our algorithm using simulationaly-generated sphere (Fig. 5 (a)), which is

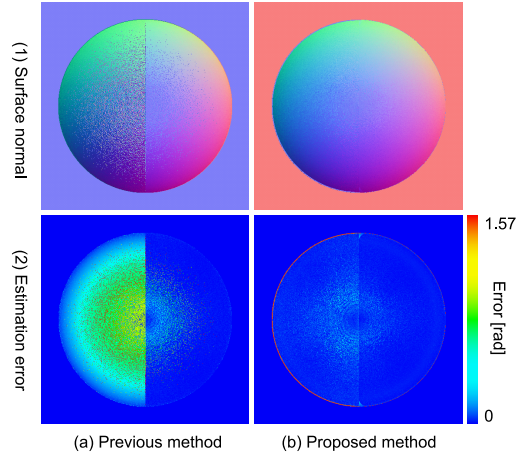


Figure 6. Comparison between (a) previous method and (b) proposed method: (1) Computed surface normal and (2) angular error between estimated surface normal and true surface normal.

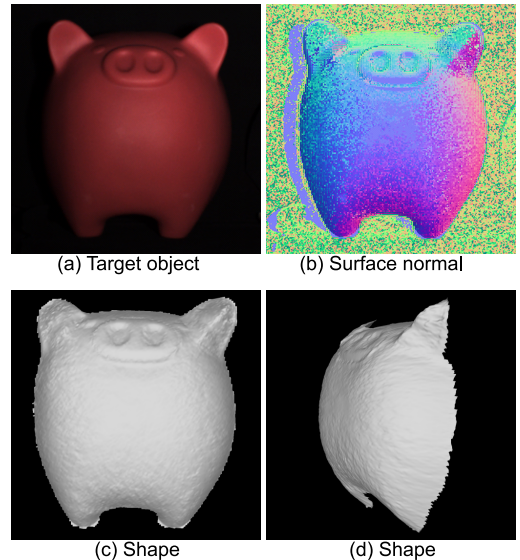


Figure 7. Experimental result [pig]: (a) Target object, (b) estimated surface normal, and (c) (d) reconstructed shape.

multi-colored. The input polarization data with noise added is shown in Fig. 5 (b) in pseudo color whose hue represents the orientation. The estimated surface normal of the previous method [14] and the proposed method is shown in Fig. 6 (1a) and Fig. 6 (1b), respectively. Surface normal is represented by pseudo color, where x , y , and z represents R, G, and B, respectively. The error between the estimated normal and the true normal is shown in Fig. 6 (2a) and Fig. 6 (2b), respectively. The average error of previous method is 0.309 [rad] and that of our method is 0.078 [rad]. The result

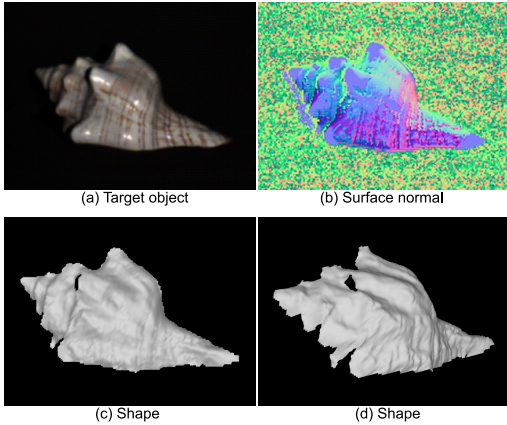


Figure 8. Experimental result [shell]: (a) Target object, (b) estimated surface normal, and (c) (d) reconstructed shape.

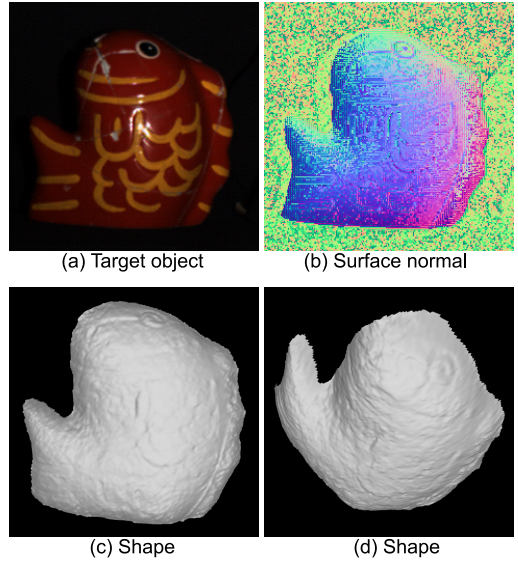


Figure 10. Experimental result [fish]: (a) Target object, (b) estimated surface normal, and (c) (d) reconstructed shape.

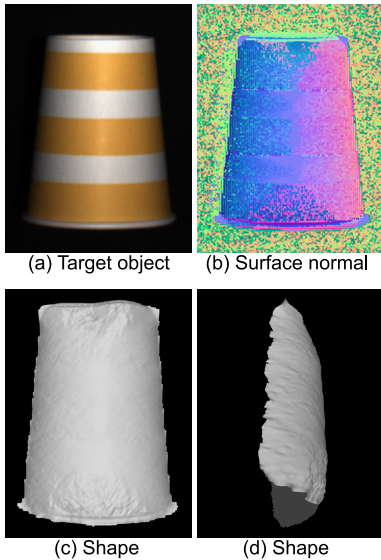


Figure 9. Experimental result [cup]: (a) Target object, (b) estimated surface normal, and (c) (d) reconstructed shape.

shows that the performance of our method is higher than that of previous method. Our method can be applied to multi-colored object.

4.2 Experimental results

We applied our method to objects shown in Figs. 7 (a), 8 (a), 9 (a), and 10 (a), whose shapes look like a pig, a shell, a cup, and a fish, respectively. The objects shown in Figs. 7 (a) and 8 (a) are single-colored, while those shown in Figs. 9 (a) and 10 (a) are multi-colored. The estimated surface normals are shown in Figs. 7 (b), 8 (b), 9 (b), and 10 (b), respectively. The reconstructed

shapes are shown in Figs. 7 (c) (d), 8 (c) (d), 9 (c) (d), and 10 (c) (d), respectively. These figures show that our method successfully estimated the shape of the object.

Although the guide normal cannot represent the detail of the shape, our method can recover the details of the shape, as is shown in the nose of Fig. 7, and the thorn of Fig. 8. However, as is shown in the top rim and the bottom rim of the cup shown in Fig. 9, the shape which is different from the guide normal is difficult to solve. Such dilemma is difficult to solve fundamentally, and it is our challenging future work.

5 Conclusion

We have proposed a method which estimates the surface normal from shading, polarization, and silhouette. Approximate shape calculated from silhouette is used as a cue. Shading information constrain the z-axis of surface normal. Polarization information constrain the x- and y-axes of surface normal. The experimental results show that our method can estimate the shape of multi-colored object from a single image.

Our future work is to use additional input, additional constraint, or additional training data so that we can estimate the shapes which are quite different from the guide normal.

References

- [1] B. K. P. Horn and M. J. Brooks, "The variational approach to shape from shading," *Computer Vision, Graphics, and Image Processing*, vol. 33, no. 2, pp. 174–208, 1986.
- [2] R. Zhang, P. S. Tsai, J. E. Cryer, and M. Shah, "Shape-from-shading: a survey," *IEEE Transactions on Pattern Analysis and Machine Intelligence*, vol. 21, no. 8, pp. 690–706, 1999.
- [3] J.-D. Durou, M. Falcone, and M. Sagona, "Numerical methods for shape-from-shading: A new survey with benchmarks", *Computer Vision and Image Understanding*, vol. 109, no. 1, pp. 22–43, 2008.
- [4] B. K. P. Horn, "Obtaining shape from shading information," *The Psychology of Computer Vision*, pp. 115–155, 1975.
- [5] B. K. P. Horn, "Height and gradient from shading," *International Journal of Computer Vision*, vol. 5, pp. 37–75, 1990.
- [6] T. Rindfleisch, "Photometric method for lunar topography," *Photogrammetric Engineering*, vol. 32, no. 2, pp. 262–277, 1966.
- [7] M. Born and E. Wolf, *Principles of optics*, Pergamon Press, London, 1959.
- [8] G. A. Atkinson and E. R. Hancock, "Surface reconstruction using polarization and photometric stereo," in *Computer Analysis of Images and Patterns*, 2007.
- [9] O. Drbohlav and R. Sara, "Unambiguous determination of shape from photometric stereo with unknown light sources," in *IEEE International Conference on Computer Vision*, vol. 1, pp. 581–586, 2001.
- [10] T. T. Ngo, H. Nagahara, and R. Taniguchi, "Shape and light directions from shading and polarization," in *IEEE Conference on Computer Vision and Pattern Recognition*, pp. 2310–2318, 2015.
- [11] S. Tozza, W. A. P. Smith, D. Zhu, R. Ramamoorthi, E. R. Hancock, "Linear differential constraints for photopolarimetric height estimation," in *IEEE International Conference on Computer Vision*, pp. 2298–2306, 2017.
- [12] F. Logothetis, R. Mecca, F. Sgallari, and R. Cipolla, "A differential approach to shape from polarisation: A level-set characterisation," *International Journal of Computer Vision*, vol. 127, pp. 1680–1693, 2019.
- [13] D. Miyazaki and S. Hashimoto, "Uncalibrated photometric stereo refined by polarization angle," *Optical Review*, vol. 28, pp. 119–133, 2021.
- [14] N. Kodama, "—," *Graduation Thesis*, Hiroshima City University, 2020. (in Japanese)
- [15] A. H. Mahmoud, M. T. El-Melegy, and A. A. Farag, "Direct method for shape recovery from polarization and shading," in *IEEE International Conference on Image Processing*, pp. 1769–1772, 2012.
- [16] S. Tozza, W. A. P. Smith, D. Zhu, R. Ramamoorthi, and E. R. Hancock, "Linear differential constraints for photo-polarimetric height estimation," in *IEEE International Conference on Computer Vision*, pp. 2298–2306, 2017.
- [17] W. A. P. Smith, R. Ramamoorthi, and S. Tozza, "Height-from-polarisation with unknown lighting or albedo," *IEEE Transactions on Pattern Analysis and Machine Intelligence*, vol. 41, no. 12, pp. 2875–2888, 2019.